



Fachhochschule Köln
Cologne University of Applied Sciences



UNIVERSIDAD AUTÓNOMA DE SAN LUIS POTOSÍ
FACULTADES DE CIENCIAS QUÍMICAS, INGENIERÍA Y MEDICINA
PROGRAMAS MULTIDISCIPLINARIOS DE POSGRADO EN CIENCIAS AMBIENTALES

AND

COLOGNE UNIVERSITY OF APPLIED SCIENCES
INSTITUTE FOR TECHNOLOGY AND RESOURCES MANAGEMENT IN THE TROPICS AND SUBTROPICS

ADSORPTION KINETICS MODELING OF A RED AZO DYE ONTO BONE CHAR

THESIS TO OBTAIN THE DEGREE OF

MAESTRÍA EN CIENCIAS AMBIENTALES

DEGREE AWARDED BY

UNIVERSIDAD AUTÓNOMA DE SAN LUIS POTOSÍ

AND

MASTER OF SCIENCE

TECHNOLOGY AND RESOURCES MANAGEMENT IN THE TROPICS AND SUBTROPICS

IN THE SPECIALIZATION: RESOURCES MANAGEMENT

DEGREE AWARDED BY COLOGNE UNIVERSITY OF APPLIED SCIENCES

PRESENTS:

DOUGLAS OSWALDO PINO HERRERA

CO-DIRECTOR OF THESIS PMPCA

DR. LUIS ARMANDO BERNAL JÁCOME

CO-DIRECTOR OF THESIS ITT:

DR. MICHAEL STURM

ASSESSOR:

DR. ANTONI ESCALAS CAÑELLAS



Fachhochschule Köln
Cologne University of Applied Sciences



UNIVERSIDAD AUTÓNOMA DE SAN LUIS POTOSÍ
FACULTADES DE CIENCIAS QUÍMICAS, INGENIERÍA Y MEDICINA
PROGRAMAS MULTIDISCIPLINARIOS DE POSGRADO EN CIENCIAS AMBIENTALES
AND
COLOGNE UNIVERSITY OF APPLIED SCIENCES
INSTITUTE FOR TECHNOLOGY AND RESOURCES MANAGEMENT IN THE TROPICS AND SUBTROPICS

ADSORPTION KINETICS MODELING OF A RED AZO DYE ONTO BONE CHAR

THESIS TO OBTAIN THE DEGREE OF
MAESTRÍA EN CIENCIAS AMBIENTALES
DEGREE AWARDED BY
UNIVERSIDAD AUTÓNOMA DE SAN LUIS POTOSÍ
AND
MASTER OF SCIENCE
TECHNOLOGY AND RESOURCES MANAGEMENT IN THE TROPICS AND SUBTROPICS
IN THE SPECIALIZATION: RESOURCES MANAGEMENT
DEGREE AWARDED BY COLOGNE UNIVERSITY OF APPLIED SCIENCES

PRESENTS:

DOUGLAS OSWALDO PINO HERRERA

DR. LUIS ARMANDO BERNAL JÁCOME

DR. MICHAEL STURM

DR. ANTONI ESCALAS CAÑELLAS

**PROYECTO FINANCIADO POR:
PROMEP/103-5/09/300 Y ENREM-DAAD 2012 PARTIDA 2.4/5**

PROYECTO REALIZADO EN:

PMPCA

FACULTAD DE INGENIERÍA

UNIVERSIDAD AUTÓNOMA DE SAN LUIS POTOSÍ

CON EL APOYO DE:

**DEUTSCHER AKADEMISCHER AUSTAUSCH DIENST (DAAD)
CONSEJO NACIONAL DE CIENCIA Y TECNOLOGÍA (CONACYT)**

**LA MAESTRÍA EN CIENCIAS AMBIENTALES RECIBE APOYO A TRAVÉS DEL PROGRAMA
NACIONAL DE POSGRADOS (PNPC - CONACYT)**

Erklärung / Declaración

Name / *Nombre*: Douglas Oswaldo Pino Herrera

Matri.-Nr. / *N° de matricula* 11090037 (CUAS), 0204036 (UASLP)

Ich versichere wahrheitsgemäß, dass ich die vorliegende Masterarbeit selbstständig verfasst und keine anderen als die von mir angegebenen Quellen und Hilfsmittel benutzt habe. Alle Stellen, die wörtlich oder sinngemäß aus veröffentlichten und nicht veröffentlichten Schriften entnommen sind, sind als solche kenntlich gemacht.

Aseguro que yo redacté la presente tesis de maestría independientemente y no use referencias ni medios auxiliares a parte de los indicados. Todas las partes, que están referidas a escritos o a textos publicados o no publicados son reconocidas como tales.

Die Arbeit ist in gleicher oder ähnlicher Form noch nicht als Prüfungsarbeit eingereicht worden.

Hasta la fecha, un trabajo como éste o similar no ha sido entregado como trabajo de tesis.

San Luis Potosí, den /*el* _____

Unterschrift / *Firma*: _____

Ich erkläre mich mit einer späteren Veröffentlichung meiner Masterarbeit sowohl auszugsweise, als auch Gesamtwerk in der Institutsreihe oder zu Darstellungszwecken im Rahmen der Öffentlichkeitsarbeit des Institutes einverstanden.

Estoy de acuerdo con una publicación posterior de mi tesis de maestría en forma completa o parcial por las instituciones con la intención de exponerlos en el contexto del trabajo investigación de las mismas.

Unterschrift / *Firma*: _____

ACKNOWLEDGEMENT

Quisiera agradecer a todas las personas que hicieron posible la realización de este proyecto. A mis codirectores el Dr. Luis Armando Bernal y el Dr. Michael Sturm por su guía y apoyo. Así mismo, a mi asesor el Dr. Antoni Escalas por ser un excelente anfitrión en mi estancia en Terrassa y por toda su ayuda.

Muchas gracias a las personas que hicieron mi trabajo más fácil en la fase experimental de mi tesis. Al Dr. Roberto Leyva Ramos por facilitarme el equipo necesario y sus enseñanzas y al laboratorio de Tratamiento de Aguas Residuales de la Facultad de Ingeniería de la UASLP por el espacio y los instrumentos de trabajo. Gracias a Yvette y a Alejandra por su ayuda en el laboratorio.

A mis profesores de maestría por toda la enseñanza y sabiduría impartida.

Agradecimientos especiales van a mi familia. A mi madre Mirna Herrera, por su apoyo constante y su preocupación en todo momento de mi vida. A mis hermanos Daniela y Daniel por siempre estar ahí cuando los necesito e impulsarme y servir de ejemplo para ser mejor profesional y persona. A mi padre, Daniel Pino, por estar pendiente de mi evolución y su disposición a siempre ayudarme. A mis abuelos por estar atentos a mis pasos en cada momento de mi vida.

A mis compañeros de maestría y especialmente a los amigos, que pasaron a formar parte de mi familia durante estos dos años de travesía juntos. Muchas gracias por tantos momentos juntos: buenos, malos, bonitos y no tan bonitos. ¡Nos vemos pronto muchachieren!

Finalmente, quisiera agradecerle a una persona que aprecio y quiero mucho y que en los últimos meses ha estado cerca de mí, apoyándome, dándome ánimo, que me ha hecho un poco más fácil esta etapa de mi vida, que me ha recordado que en todo hay un aprendizaje y que me ha recordado, en sus propias palabras, que todo se puede lograr con paciencia y mucha perseverancia.

ABSTRACT

Colored wastewater could arise as a direct result of the production of dyes and also as a consequence of its use in the textile and other industries (Allen & Koumanova, 2005). Aromatic amines are used in the fabrication of azoic dyes and, when dyes are degraded these compounds are regenerated as a consequence of the azo bond rupture. Some aromatic amines can be carcinogenic. That means that it is necessary to remove the dyes from the wastewater (Martínez, 2011). For this purpose, the best technology available is adsorption. Few earlier studies have demonstrated the capacity of bone char to adsorb dyes (Bernal, 2011).

The main objective of this project is to study and to model the adsorption kinetics of a red azo dye onto bone char, in order to obtain data that can be used in future projects for the removal of dyes in textile and other industries wastewater.

Several experiments were carried out varying system conditions, such as, initial concentration, bone char mass and stirring speed. The concentration decay curve was obtained for each experiment.

A theoretical diffusion model with four variations was used to predict the behavior of the system. The parameters that were used to fit the model were: external mass transfer coefficient, effective pore diffusivity and effective surface diffusivity. The variations of the diffusion model were: Film- pore diffusion model (FPD), Film- surface diffusion model (FSD), Film- pore- unique surface diffusion model (FPUSD) and Film- pore- initial conditions dependent surface diffusion model (FPICDSD). The equations of the model were solved using the computer program PDESOL.

As results, this study found out that FPICDSD model was the one which best fit to the parameters with an Overall Average Relative Error of 0.99% approximately. It was also proved that the effective surface diffusivity has an exponential relation with the mass of solute adsorbed at equilibrium for the initial conditions of the system.

RESUMEN

Las aguas residuales con colorante pueden surgir como resultado directo de la producción de colorantes o como consecuencia de su uso en la industria (Allen & Koumanova, 2005). En la fabricación de colorantes azo se utilizan aminas aromáticas. La degradación de estos colorantes puede producir de nuevo estos compuestos, debido a la ruptura del enlace azo y algunas de estas aminas aromáticas pueden ser carcinógenas. Esto significa que es necesario remover este tipo de colorantes de las aguas residuales (Martínez, 2011). Para este propósito, la mejor tecnología disponible es la adsorción. Algunos estudios previos han demostrado la capacidad del carbón de hueso de adsorber colorantes (Bernal, 2011).

Es por eso que el principal objetivo de este proyecto es estudiar y modelar la cinética de adsorción de un colorante azo rojo sobre carbón de hueso, con el propósito de obtener información útil que pueda servir a futuros proyectos en la remoción de colorantes en las aguas residuales de la industria textil y otras industrias.

Varios experimentos fueron llevados a cabo en un sistema de adsorción tipo batch, variando las condiciones, tales como, concentración inicial, masa de adsorbente y velocidad de agitación. Fue obtenida la curva de decaimiento de concentración en la solución para cada experimento.

Fue utilizado un modelo teórico difusional con cuatro variaciones para predecir el comportamiento del sistema. Los parámetros a ajustar fueron: coeficiente de transferencia de masa externo, difusividad efectiva en el volumen del poro y difusividad efectiva en la superficie. Las variaciones del modelo teórico difusional fueron: el modelo de difusión de película-volumen del poro, modelo de difusión de película-superficie, modelo de difusión de película-volumen del poro-superficie con difusividad superficial única y modelo de difusión de película-volumen de poro-superficie con difusividad superficial dependiente de condiciones iniciales. Las ecuaciones del modelo fueron resueltas utilizando el programa PDESOL.

Como resultado se obtuvo que el modelo de difusión de película-volumen de poro-superficie con difusividad superficial dependiente de condiciones iniciales fue el que mejor ajustó a los parámetros con un Error Relativo Promedio global de aproximadamente 0.99%. También se pudo comprobar que la difusividad superficial efectiva, para este modelo, tiene una relación exponencial con la masa de soluto adsorbida en el equilibrio para las condiciones iniciales del sistema.

TABLE OF CONTENT

ACKNOWLEDGEMENT	i
ABSTRACT	ii
RESUMEN	iii
NOMENCLATURE	v
CHAPTER 1: INTRODUCTION	1
CHAPTER 2: DYES AND BONE CHAR	4
2.1 Dyes	4
2.1.1 Dyes classification	4
2.1.2 Azo dyes.....	6
2.2 Bone char	7
CHAPTER 3: ADSORPTION	8
3.1 Adsorption kinetics	9
3.1.1 Adsorption kinetics modeling.....	10
3.1.2 Diffusion model.....	12
CHAPTER 4: METHODOLOGY	16
4.1 Experimental phase	16
4.2 Modeling phase	18
4.2.1 Film- Pore diffusion model (FPD).....	18
4.2.2 Film- Surface diffusion model (FSD).....	19
4.2.3 Film- Pore- Surface diffusion model (FPSD)	19
CHAPTER 5: EXPERIMENTAL DATA	21
CHAPTER 6: CALCULATIONS, RESULTS AND DISCUSSION	24
6.1 Equilibrium data.....	26
6.2 External mass transport coefficient calculation	26
6.3 External mass transport coefficient effect on the system.....	28
6.4 Diffusivities calculation	29
6.4.1 Film- Pore diffusion model (FPD).....	31
6.4.2 Film- Surface diffusion model (FSD).....	32
6.4.3 Film- Pore- Surface diffusion model (FPSD)	33
CHAPTER 7: CONCLUSIONS	38
REFERENCES	39

NOMENCLATURE

ARE	Average relative error, %
C_A	Solute concentration in bulk solution, mg/cm ³
C_{A0}	Initial adsorbate concentration in the aqueous solution, mg/ml
$C_{A,r}$	Adsorbate concentration in the pore at a r distance,mg/ml
C_{AS}	Adsorbate adsorption concentration on the adsorbent surface, mg/cm ³
C_e	Bulk concentration at equilibrium, mg/l
D_e	Effective diffusivity, cm ² /s
$D_{e,p}$	Effective diffusivity coefficient in the pore,cm ² /s
$D_{e,s}$	Effective surface diffusion,cm ² /s
D_{s0}	Surface diffusivity at $C_e=0$, cm ² /s
k_c	External mass transfer coefficient, cm/s
k_F	Freundlich equation constant
m	Adsorbent particle mass, g
N	Number of experiments for ARE
n	Freundlich equation constant
N_A	Solute A mass flow, mg/cm ² s
$N_{A,p}$	Mass flow due to molecular diffusion mg/cm ² s
$N_{A,s}$	Mass flow due to surface diffusion, mg/cm ² s
q	Adsorbate amount per adsorbent mass, mg/g
q_e	Solute mass adsorbed at equilibrium, mg/g
r	Distance in the diffusion direction, cm.
S	External surface area per adsorbent mass,cm ² /g
t	Time, s
V	Aqueous solution volume, ml

GREEK SYMBOLS

ε_p	Adsorbent porosity
ϕ	Non-dimensional bulk concentration at a specific time
ρ_p	Adsorbent particle density, g/cm ³

CHAPTER 1: INTRODUCTION

The textile industry is the economic sector dedicated to the production of yarn, fabric, clothing, fiber and related products. The manufacture of the different textile products is carried out by processes such as cleaning, stretching, dyeing, etc. Due to this processes, the textile industry generates wastewater with a great number of pollutants, among which dyes can be found. The degradation of these compounds is not easy.

Colored wastewater could arise as a direct result of the production of dyes and also as a consequence of its use in the textile and other industries. It is estimated that 2% of the dyes produced annually are discharged in effluent from manufacturing operations, whilst 10% are discharged from textile and associated industries (Allen & Koumanova, 2005).

Aromatic amines are used in the fabrication of azoic dyes and when dyes are degraded, these compounds are regenerated as a consequence of the azo bond rupture. Some aromatic amines can be carcinogenic. That means that it is necessary to remove the dyes from the wastewater (Martínez, 2011).

For this purpose, the best technology available is adsorption. Normally, activated carbon is used as adsorbent, but other materials can be used as well, for example bone char.

To design an adsorption process it is necessary to know the breakthrough curve of the column. The breakthrough curve is the “S” shaped curve that typically results when the effluent adsorbate concentration is plotted against time or volume treated (Figure 1).

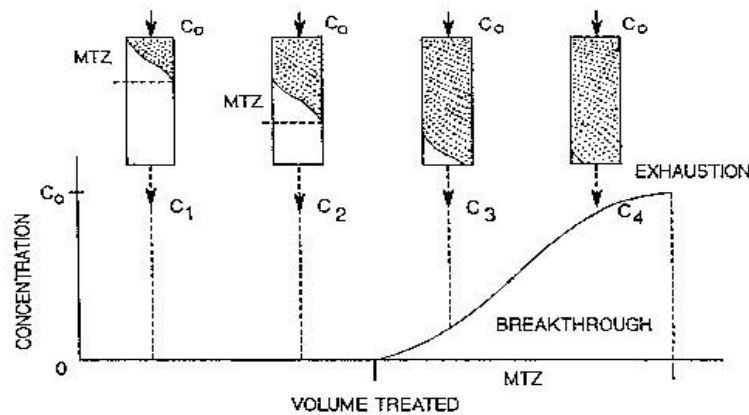


Figure 1. Example of breakthrough curve (Wu, 2004)

It is possible to predict the breakthrough curve. If the curves for adsorption processes can be reliably predicted and easily determined, laboratory measurements and extensive pilot plant scale studies can be obviated and considerable savings in time and money can be achieved. This supposes the application of appropriate mathematical modeling techniques for operation on information developed from component and condition analysis (Weber, 1972).

In the Figure 2, it can be seen that the prediction is generally good for the first 50 - 60% of the operational period of the adsorber. Usually, this is enough for most practical purposes, since adsorption processes are normally not operated to more than 15 -30% breakthrough in wastewater treatment.

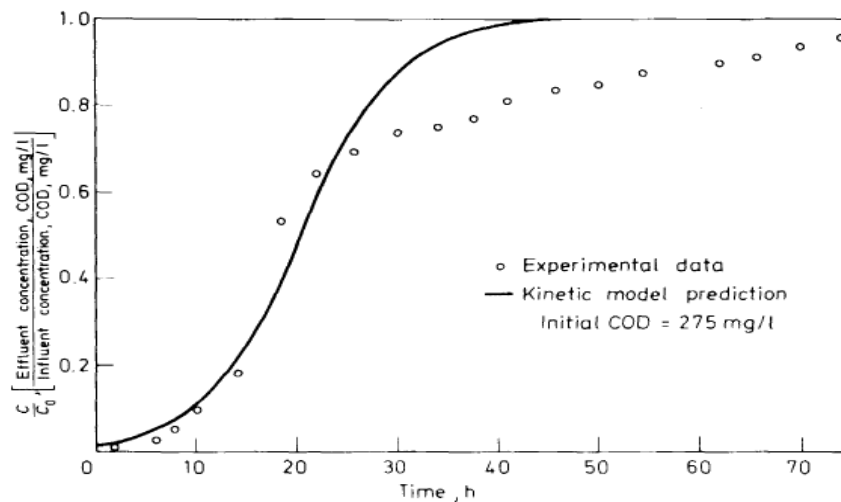


Figure 2. Breakthrough curve prediction with kinetic modeling (Weber, 1972)

There are many studies on the adsorption of dyes onto activated carbon. Although, it is known that bone char has been used historically to eliminate colored compounds, its utilization is not very frequent to adsorb dyes.

Because of this, the main objective of this project is to study and to model the adsorption kinetics of a red azo dye onto bone char, in order to obtain data that can be used in future projects for the removal of dyes in textile and other industries wastewater.

In order to reach the main goal, the following next specific objectives were proposed:

- To obtain experimental data of adsorption kinetics of the azoic red onto bone char.
- To analyze the obtained data and to fit parameters for a diffusion model in order to define the variables that control the process.

It is important to remark that this project is part of a bigger project named “Optimization of adsorbents used for dye removal in textile wastewater”.

CHAPTER 2: DYES AND BONE CHAR

2.1. Dyes

Dyes are substances, which are applied to a substrate (fibers, textiles, leather, paper, polymers, food), whether in solution or in dispersion, and give to it a color more or less permanent. The substrate should have certain chemical affinity to it, in order to retain it (Zoolilinger, 2001).

The principal characteristics that a dye should have are:

- Color
- Light resistance
- Substrate adherence (wash and wear resistance)
- Color uniformity in a wide surface
- Harmless for the substrate

2.1.1. Dyes Classification

Dyes can be classified according to two different criteria (Wittcoff & Reuben, 1980):

i. Classification by the chromophore group

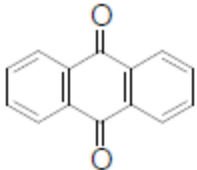
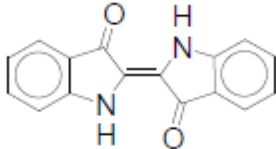
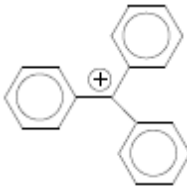
The chromophore group is the part of the molecular structure that absorbs and then emits radiation, which gives the color. Normally, it is a double bond conjugated system, which often has heteroatoms (i.e. N, S, P, metals). Besides these groups, there are other groups in the dye molecule that are capable of extending this system and changing the original color.

There are more than twelve families of dyes. However, the most important four groups for the industry are shown in Table 1.

ii. Classification by functional properties and application way

According to their properties and application ways in the dyeing of the substrate, the dyes are grouped in these categories: direct, disperse, vat, mordant, acid and basic, reactive, among others.

Table 1. Families of the most important dyestuffs

Name of the family	Chromophore group
Azoic	Ar-N=N-Ar
Anthraquinones	<p data-bbox="889 415 1019 447">Azo group</p> 
Indolic	<p data-bbox="862 684 1047 716">Anthraquinone</p> 
Dyestuff of triarylmethane	<p data-bbox="915 926 993 957">Indigo</p> 
	Triphenylmethyl cation

- **Direct dyes:** they are simply applied by the immersion of the substrate in a neutral and hot solution containing the dyestuff and which previously has been added an electrolyte.
- **Disperse dyes:** they are insoluble in water and are applied using colloidal dispersions of the dye in water. The precipitate particles of the dye are adhered to the fiber by dipolar interactions.
- **Soluble in organic solvents dyes:** they are used for wood, ink, gasoline, oils and plastics. Normally, they are anthraquinones.
- **Vat dyes:** In this case, the dye is added in an inactive, reduced, colorless form, very soluble in water. Then, it is oxidized, becoming much less soluble in water. Therefore, it precipitates and binds to the substrate.

- **Acid or basic dyes:** the acid (anionic) and basic (cationic) dyes are used for dyeing fabrics, which have positive acid or negative basic groups on the surface. This is the case, for example, of wool or silk. The dyestuff is bonded to substrate by polar forces, forming salts.
- **Mordant dyes:** they are used in conjunction with a mordant, which normally is a metallic salt. This salt forms an insoluble complex with the dye. They are usually from the azoic or antraquinone group.
- **Reactive dyes:** They are fixated to the substrate by a covalent bond, which makes them very resistant to washing. Usually, they have trichlorotriazine group, which reacts through one of the chlorine atoms with the substrate. This procedure is more expensive than the others, but it is very effective.

2.1.2. Azo dyes

As it was explained previously, azoic dyes have as chromophore an azo group jointed to two aryl groups (Ar-N=N-Ar). A great amount of world dye production is azoic (between 40-50%). In fact, the main dyes used worldwide in the textile, paper, food, cosmetic and pharmaceutical industries are the azoic kind, and there are near 3000 types of them (Quezada & Buitrón, s.f.).

The structural formula of Reactive Remazol Red 24 is shown in Figure 3. This represents an example of this type of dyes. In aqueous solution, this molecule ionizes, forming an anion.

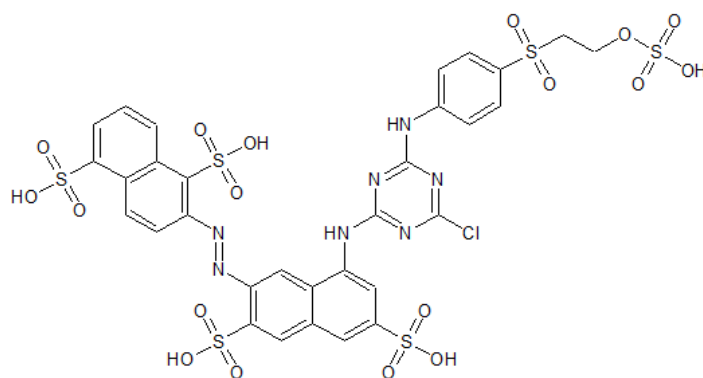


Figure 3. Reactive Remazol Red 241

2.2. Bone char

Bone char is a material obtained by carbonizing animal bones. It consists mainly of hydroxiapatite [$\text{Ca}_{10}(\text{PO}_4)_6(\text{OH})_2$] (80 – 90%), and carbon to a lesser degree (4 – 10%). Bone char is used usually to adsorb some anions like fluoride, arsenate, dichromate, etc or some cations like Sr^{+2} , Pb^{+2} , among others. It has its zero charge point between pH 8 and 9. Figure 4 shows the possible ways of the surface ionization in bone char.

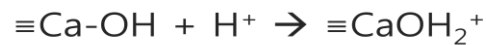
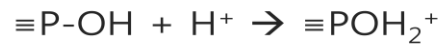
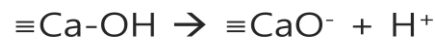


Figure 4. Possible ways of ionization of the bone char

There are many studies on the adsorption of dyes onto activated carbon. Although, it is known that bone char has been used historically to eliminate colored compounds, its utilization is not very frequent to adsorb dyes.

Bernal et al. (2011) have made a study of the adsorption equilibrium of a red azo dye onto bone char. The results of this study will be used for the adsorption kinetics modeling of this project.

CHAPTER 3: ADSORPTION

Adsorption consists in the transfer of an adsorbate from a gas or liquid phase to an adsorbent, where it binds through intermolecular forces (see Figure 5). This phenomenon is applied in processes of gases purification, such as removal of sulfur dioxide from a chimney and as a way to separate liquids hard to isolate using other methods. Oil and chemical industries use widely adsorption for water and wastewater treatment and purification and for gases dehydration. The quantity of adsorbate that can be collected in a surface area unit is small. Because of this, normally porous adsorbents with a great internal surface area are selected. Some examples of adsorbents that have this characteristics are activated carbon, silica gel, activated alumina, zeolites, clays, etc. (Hines & Maddox, 1987).

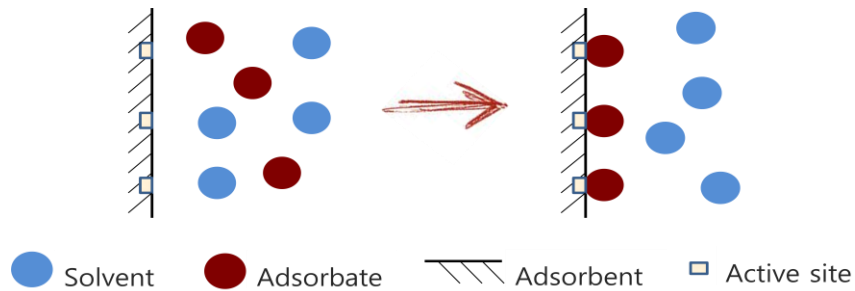


Figure 5. Illustration of the adsorption phenomenon

Two types of adsorption phenomena can be told apart: physical and chemical. Physical adsorption, easily reversible, is the result of Van der Waals intermolecular forces between adsorbent and adsorbed substance. These interactions are far-reaching, but weak, thus the energy when the molecule is physisorbed is about the same order of magnitude as the condensation enthalpy. When this condensation occurs, a certain amount of heat is released, which generally is a little higher than the evaporation latent heat and is alike to the sublimation heat of the gas.

On the other hand, according to Treybal (2002), chemisorption is the result of the chemical interaction between the solid and the substance adsorbed. The chemical bond formed between the adsorbate and the adsorbent is usually covalent (Atkins & De Paula, 2003).

The chemical bond force can considerably vary and chemical compounds cannot be formed in the usual way. However, the adhesion forces are normally a lot higher than those observed in physisorption. The heat released during chemisorption, which always is an exothermic process, is commonly high and is similar to a chemical reaction heat. The same substance that at low temperatures experiences essentially physical adsorption onto a solid, sometimes exhibits chemical adsorption at higher temperatures. Sometimes both processes can occur simultaneously (Treybal, 2002).

3.1. Adsorption Kinetics

Adsorption kinetics is a thermodynamic approach that describes the relation between the adsorbed species and the fluid free phase. The adsorption rate depends on the number of particles striking the surface per time unit and on the so-called sticking coefficient, which is the probability that an incident particle actually adheres to the substrate (Lüth, 2010).

The kinetic analysis of the adsorption may set up the solute uptake rate, which determines the residence time required for completion of adsorption. Kinetic information can also give the scale of an adsorption apparatus. In general, adsorption kinetics is the base to determine the performance of fixed-bed or any other flow-through system (Qiu, 2009).

The transfer of a compound from a liquid phase to an adsorption site occurs in four steps, as it is shown in the Figure 6 (Dudamel, et al., 2010): First, the compound transfer from the liquid to the film near the adsorbent happens (quick stage).

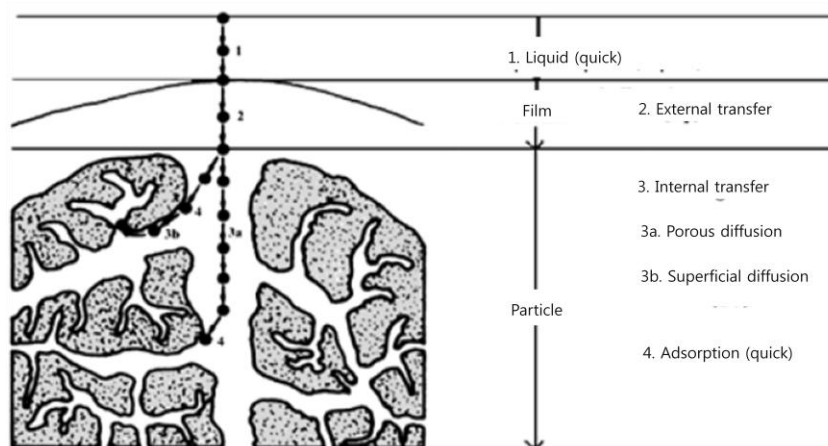


Figure 6. Adsorption process stage (Dudamel, et al., 2010)

Then, the compound transfer through the film near the external surface of the adsorbent occurs (external mass transfer). Next, the compound is diffused into the adsorbent particle (intraparticle diffusion) in two possible ways: in the volume of the pore or along the surface.. Finally, the proper adsorption occurs, and this is a quick stage too. The adsorption kinetics is determined by the slowest stage.

3.1.1. Adsorption kinetic modeling

Several mathematical models have been proposed to represent the global process of adsorption on porous adsorbents. Qiu et al. (2009) summarize the principal kinetic models used nowadays and classify them into three categories: adsorption reaction models, adsorption diffusion models and a third model named Double-exponential model (DEM). However, most of these models only consider the pore volume diffusion or the surface diffusion or they do not take into account the adsorbate mass that accumulates in the solution inside pores (Bernal & Leyva, 1999).

A more general theoretical model has been proposed, which includes both mechanisms of intraparticle diffusion and the external mass transport, as follows (Geankopolis & Leyva-Ramos, 1985):

- i. External mass transport is represented by the film theory (Equation 3.1)

$$N_A = k_c(C_A - C_{AS}) \quad (3.1)$$

Where:

N_A : Solute A mass flow, mg/cm² s

k_c : External mass transfer coefficient, cm/s

C_A : Solute A concentration in bulk solution, mg/cm³

C_{AS} : adsorbate A adsorption concentration just in the adsorbent surface, mg/cm³.

- ii. Intraparticle transport may occur by pore volume molecular diffusion, by surface diffusion or a combination of both mechanisms. The pore volume molecular diffusion is evaluated by an equation similar to the Fick Law (Equation 3.2).

$$N_{A,p} = -D_{e,p} \frac{dC_{A,r}}{dr} \quad (3.2)$$

Where:

$N_{A,p}$: Mass flow due to molecular diffusion in the adsorbent pore, mg/cm² s

$D_{e,p}$: Effective diffusivity coefficient in the pore, cm²/s

$C_{A,r}$: Adsorbate concentration in the pore at a r distance, mg/ml

r : Distance in the diffusion direction, cm.

The mass transport due to surface diffusion can also be represented by an equation similar to the Fick Law, but using an adsorbed solute concentration gradient onto the pore surface (Equation 3.3)

$$N_{A,s} = -D_{e,s} \rho_p \frac{dq}{dr} \quad (3.3)$$

Where:

$N_{A,s}$: Mass flow due to surface diffusion, mg/cm² s

$D_{e,s}$: Effective surface diffusion, cm²/s

q : Adsorbate amount per adsorbent mass, mg/g

ρ_p : Adsorbent particle density, g/cm³

Adsorption onto an active site is generally considered as an instantaneous process. Therefore, it is represented by the isotherm adsorption.

3.1.2. Diffusion model

In this section, the model used in this study will be developed. In order to do that, a system in which a certain amount of bone char gets in touch with an aqueous solution of red azo dye with constant volume and determined concentration. In this system, two regions are considered: the constant volume aqueous solution and the porous of the bone char particles (Bernal & Leyva, 1999).

To develop the model, first, a mass balance of the adsorbate in the aqueous solution is made, from which an ordinary differential equation (Equation 3.4) and its respective initial condition (Equation 3.5) is obtained (Geankopolis & Leyva-Ramos, 1985).

$$V \frac{dC_A}{dt} = -mSk_c(C_A - C_{AS}) \quad (3.4)$$

$$\text{When } t = 0 ; C_A = C_{A0} \quad (3.5)$$

Where:

m : Adsorbent particle mass, g

V : Aqueous solution volume, ml

S : External surface area per adsorbent mass, cm^2/g

C_{A0} : Initial adsorbate concentration in the aqueous solution, mg/ml

t : Time, s

The left side term of the Equation 3.4 represents the adsorbate concentration diminution rate in the aqueous solution due to the adsorption onto the adsorbent adsorption and the right side term shows the diffusion rate of the adsorbate from the bulk solution to the particle surface.

Then, a mass balance of the adsorbate in the adsorbent particle is made on a differential element, assuming that the particle is spherical. This is shown in Equation 3.6.

$$\varepsilon_p \frac{\partial C_{A,r}}{\partial t} + \rho_p \frac{\partial q}{\partial t} = -\frac{1}{r^2} \frac{\partial}{\partial r} \left[r^2 (N_{A,p} + N_{A,s}) \right] \quad (3.6)$$

Where:

ε_p : Adsorbent porosity

The first term of the left side of the Equation 3.6 represents the solute accumulation in the pore and the second is the adsorbate accumulation adsorbed in the surface. Both terms in the right side are intraparticle transport due to pore and surface diffusion.

Replacing Equations 3.2 and 3.3 in Equation 3.6, Equation 3.7 is obtained.

$$\varepsilon_p \frac{\partial C_{A,r}}{\partial t} + \rho_p \frac{\partial q}{\partial t} = -\frac{1}{r^2} \frac{\partial}{\partial r} \left[r^2 \left(-D_{e,p} \frac{dC_{A,r}}{dr} + -D_{e,s} \rho_p \frac{\partial q}{\partial r} \right) \right] \quad (3.7)$$

And the respective initial and border conditions to solve it are shown in Equation 3.8, 3.9 and 3.10.

$$\left. \frac{\partial C_{A,r}}{\partial r} \right|_{r=0} = 0 \quad (3.8)$$

$$D_{e,s} \rho_p \left. \frac{\partial q}{\partial r} \right|_{r=R} + D_{e,p} \left. \frac{\partial C_{A,r}}{\partial r} \right|_{r=R} = k_c (C_A - C_{A,R}) \quad (3.9)$$

$$\text{When } t = 0 ; C_{A,r} = 0, \quad 0 \leq r \leq R \quad (3.10)$$

These boundary conditions mean that the solute mass transfer in the particle center is zero and the adsorbate mass transfer from the bulk solution to the interface equals to the mass

transfer from the interface to the particle interior. The latter condition indicates that there is no solute adsorbed at the beginning in the adsorbent.

The adsorbed amount of solute can be related to the concentration inside the particle; since the assumption of instant adsorption equilibrium is assumed.

As it was explained before, the adsorption step is a quick stage of the process, which means that the adsorbate concentration in the pore can be directly related to the adsorbate amount on the solid by the adsorption isotherm, as described in Equations 3.11 and 3.12.

$$q = f(C_{A,r}) \quad (3.11)$$

$$dq = f'(C_{A,r})dC_{A,r} \quad (3.12)$$

Freundlich isotherm is widely used for adsorption equilibrium studies. This equation and its derivative are described in Equations 3.13 and 3.14.

$$q = C_{A,r}^{1/n} \quad (3.13)$$

$$f'(C_{A,r}) = \frac{k_F}{n} C_{A,r}^{1-1/n} \quad (3.14)$$

Where k_F and n are Freundlich equation constants.

According to Cheung et al. (2006), effective diffusivity can be defined by Equation 3.15.

$$D_e = D_{e,p} + f'(C_{A,r})\rho_p D_{e,s} \quad (3.15)$$

Substituting Equations 3.14 and 3.15 equations in the mass balance, equation 3.16 is obtained.

$$\frac{\partial C_{A,r}}{\partial t} = \frac{D_e}{r^2 [\varepsilon_p + \rho_p f'(C_{A,r})]} \frac{\partial}{\partial r} \left[r^2 \frac{\partial C_{A,r}}{\partial r} \right] \quad (3.16)$$

And the corresponding border condition is represented by Equation 3.17.

$$\left. \frac{\partial C_{A,r}}{\partial t} \right|_{r=R} = \frac{k_c R}{D_e} (C_A - C_{A,R}) \quad (3.17)$$

With this definition of D_e , it is possible to develop several different theoretical models, according to the importance of the diffusion type (Cheung, et al., 2006). Table 2 shows the models used in this study.

Table 2. Models according to definition of Effective diffusivity (D_e)

Model	D_e
Film- Pore- Surface diffusion model (FPSD)	$D_e = D_{e,p} + f'(C_{A,r})\rho_p D_{e,s}$
Film- Pore diffusion model (FPD)	$D_e = D_{e,p}$
Film- Surface diffusion model (FSD)	$D_e = f'(C_{A,r})\rho_p D_{e,s}$

Also, the FPSD model may be used in two different ways: With a unique fixed surface diffusivity ($D_{e,s}$) for the whole system adsorbent-adsorbate-solvent (FPUUSD), or with different surface diffusivities dependent of the initial conditions of the system (FPICDSD).

CHAPTER 4: METHODOLOGY

In order to reach the objectives, the project was carried out in two phases: an experimental phase and a modeling phase.

4.1. Experimental phase

In this phase the necessary data to fit a model for the phenomenon was obtained. The variation of the adsorption rate in respect to time was studied, changing the initial concentration of adsorbate, the adsorbent mass and the stirring speed; all at approximately 25 °C and pH 7, as shown in the Table 2.

Table 3. Parameters studied for the adsorption kinetics modeling

Initial concentration (2 g, 100 rpm)	Adsorbent mass (400 mg/l, 100 rpm)	Stirring speed (3 g, 400mg/l)
<ul style="list-style-type: none">• 200 mg/l• 400 mg/l• 800 mg/l	<ul style="list-style-type: none">• 2 g• 3 g• 4 g	<ul style="list-style-type: none">• 100 rpm• 75 rpm• 50 rpm

A code for naming the experiments carried out in this studied was developed. It consists in 3 numbers separated by hyphens. The first number indicates the initial concentration, the second indicates the mass of bone char used and the third one is the stirring speed used. For example an experiment that was done with initial concentration of 400 mg/l approximately, 2 g of bone char and the stirring speed of 100 rpm is named “Experiment 400-2-100”. Table 4 shows the name and the initial conditions of the experiments carried out.

The experimental design, showed in the Figure 7, similar to a Carberry type reactor, consisted of a glass bowl of 1 liter of volume, in which a propeller connected to a motor was submerged. The reactor was in a controlled temperature bath and had three holes on the lid. One of them was used to submerge a pH-meter, in order to control the pH at any time in

the experiment. The other two were used to take samples and introduce makeup solution in order to maintain a constant volume in the system. The makeup solutions were prepared at an average concentration between the initial and the equilibrium concentrations in accordance with the initial conditions of the experiment. The concentration values were obtained by UV-visible spectrophotometry at 283 nm.

Table 4. Name and initial conditions of the experiments carried out in the study

Experiment name	Initial concentration (mg/l)	Bone char mass (g)	Stirring speed (rpm)
800-2-100	800	2	100
400-2-100	400	2	100
200-2-100	200	2	100
400-3-100	400	3	100
400-4-100	400	4	100
400-3-75	400	3	75
400-3-50	400	3	50

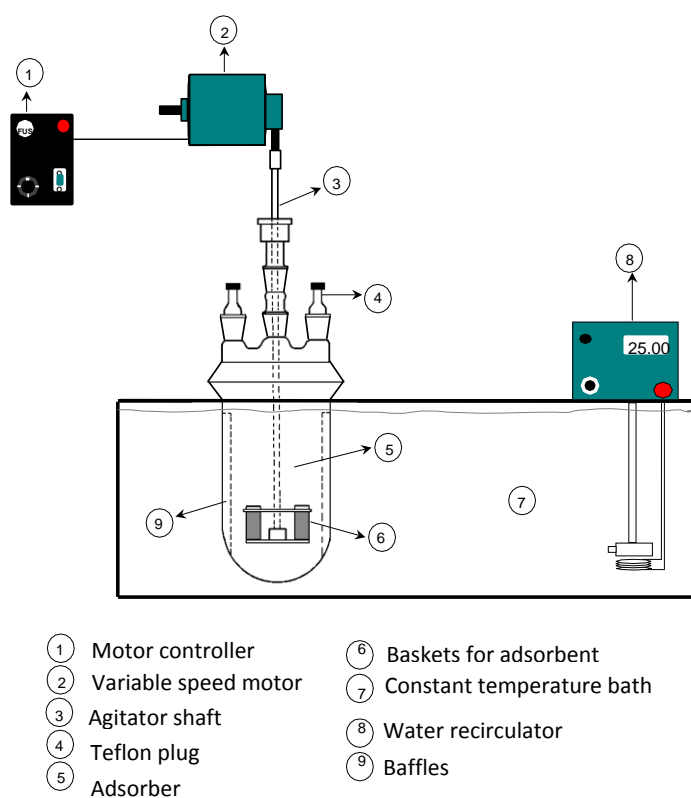


Figure 7. Experimental design

4.2. Modeling phase

The objective of the modeling phase was to determine the parameters of the theoretical model described in Chapter 3. In order to do that, the experimental data is presented as non-dimensional decay concentration curve, which is a plot of ϕ vs t . The dimensionless concentration (ϕ) is defined by Equation 4.1.

$$\phi = \frac{C_A}{C_{A0}} \quad (4.1)$$

Where:

ϕ : non-dimensional concentration at a specific time

C_A : Concentration at a specific time, mg/l

C_{A0} : Initial concentration, mg/l

Bernal (2011) have made a study of the adsorption equilibrium of the red azo dye (the one used in the current project) onto bone char. The results of this study were used for the adsorption kinetics modeling of this project.

The differential equations of the diffusion model were solved using the program PDESOL®.

The parameters to determine were the effective pore diffusivity ($D_{e,p}$) and the effective surface diffusivity, $D_{e,s}$. Four variations of the diffusion model, described before, were tested:

4.2.1. Film- Pore diffusion model (FPD)

For this case, effective surface diffusivity ($D_{e,s}$) was considered zero. The effective pore diffusivity ($D_{e,p}$) was estimated and the non-dimensional concentration decay curve was calculated. By a trial and error process, the effective pore diffusivity was changed until de best fit was found. The best fit was determined by minimizing an objective function, which was the Average Relative Error (*ARE*). *ARE* equation is shown by the equation 4.2.

$$ARE = \frac{1}{N} \sum \frac{|\phi_{exp} - \phi_{calc}|}{\phi_{exp}} \times 100\% = \text{Minimum} \quad (4.2)$$

where the subscripts *exp* and *calc* mean experimental and calculated respectively, and *N* is the experimental points number .

4.2.2. Film- Surface diffusion model (FSD)

The same procedure was applied, as the Film-Pore diffusion model, but, for this case, effective pore diffusivity ($D_{e,p}$) was fixed as zero and the variation for the trial and error process was done for the effective surface diffusivity ($D_{e,s}$).

4.2.3. Film- Pore- Surface diffusion model (FPSD)

In this case, a value for the effective diffusivity in the pore volume ($D_{e,p}$) was fixed and several values for the effective surface diffusivity ($D_{e,s}$) were tested by trial and error using as objective function the Average Relative Error (*ARE*).

Once the best fit for $D_{e,s}$ is found (for the fixed $D_{e,p}$), the value of $D_{e,p}$ is changed and the process is repeated. Several couple of values $D_{e,s}$ and $D_{e,p}$ are determined.

Now, there are two possibilities for the selection of the value(s) that represent(s) the system. The possibilities correspond to the variations of the FPSD model: when $D_{e,s}$ is the same for the whole system (FPUSD) and when it may change according to the initial conditions (FPICDSD).

i. Unique $D_{e,s}$ value (FPUSD)

The effective pore diffusivity and the corresponding effective surface diffusivity obtained from each experiment were applied as fixed values to the rest of the experimental data. Again, Average Relative Error was calculated for each experiment and each pair of diffusivities and an *Overall ARE* was calculated. The least of all the *Overall AREs* was selected as the pair of diffusivities that best fit.

ii. Initial concentration dependent $D_{e,s}$ (FPICDSD)

The effective pore diffusivity found for the experiment is fixed and the effective surface diffusivity is varied according to each experiment, until the least *ARE* is obtained. Then an *Overall ARE* is again calculated. The least *Overall ARE* is considered as the best fit and the value of $D_{e,p}$ and a set of $D_{e,s}$ values are taken for the correct values.

At the end of the process, all the *Overall ARE* calculated for each variation of the diffusion model are compared. The least one is selected as best global fit and its values of $D_{e,p}$ and $D_{e,s}$ are the main result..

CHAPTER 5: EXPERIMENTAL DATA

The experimental data for the concentration decay of the red azo dye in aqueous solution are presented from Table 3 to 9. Dimensionless concentration decay ϕ_{exp} was calculated.

Table 5. Experimental data of concentration decay of red azo dye onto bone char.
Experiment 800-2-100: Temperature= 24 °C, pH=7, stirring rate=100 rpm, bone char mass=2.0008 g.

Time (min)	Concentration (mg/l)	ϕ_{exp}
0	397.90	1.0000
1	389.60	0.9791
30	387.10	0.9729
60	380.84	0.9571
120	379.59	0.9540
180	377.09	0.9477
360	375.84	0.9446
720	369.59	0.9289
1440	357.09	0.8974
2868	349.58	0.8786

Table 6. Experimental data of concentration decay of red azo dye onto bone char.
Experiment 400-2-100: Temperature= 24 °C, pH=7, stirring rate=100 rpm, bone char mass=2.0006 g

Time (min)	Concentration (mg/l)	ϕ_{exp}
0	397.90	1.0000
1	389.60	0.9791
30	387.10	0.9729
60	380.84	0.9571
120	379.59	0.9540
180	377.09	0.9477
360	375.84	0.9446
720	369.59	0.9289
1440	357.09	0.8974
2868	349.58	0.8786

Table 7. Experimental data of concentration decay of red azo dye onto bone char.
 Experiment 200-2-100: Temperature= 24 °C, pH=7, stirring rate=100 rpm, bone char
 mass=2.0003 g

Time (min)	Concentration (mg/l)	ϕ_{exp}
0	199.86	1
1	192.43	0.9628
30	188.67	0.9440
60	186.48	0.9331
120	185.85	0.9299
180	183.97	0.9205
360	180.21	0.9017
720	177.71	0.8892
1440	171.44	0.8578
2868	166.75	0.8343

Table 8. Experimental data of concentration decay of red azo dye onto bone char.
 Experiment 400-3-100: Temperature= 24 °C, pH=7, stirring rate=100 rpm, bone char
 mass=3.0000 g

Time (min)	Concentration (mg/l)	ϕ_{exp}
0	402.71	1
1	392.81	0.9754
30	384.04	0.9536
60	376.53	0.9350
120	372.77	0.9256
180	366.50	0.9101
360	365.88	0.9085
740	358.99	0.8914
1440	345.21	0.8572
2910	337.69	0.8385

Table 9. Experimental data of concentration decay of red azo dye onto bone char.
 Experiment 400-4-100. Temperature= 25.5 °C, pH=7, stirring rate=100 rpm, bone char
 mass=4.0000 g

Time (min)	Concentration (mg/l)	ϕ_{exp}
0	399.61	1
1	383.77	0.9603
33	382.13	0.9563
60	370.08	0.9261
127	363.73	0.9102
186	358.66	0.8975
363	342.16	0.8562
728	340.25	0.8515
1458	329.47	0.8245
2880	318.05	0.7959

Table 10. Experimental data of concentration decay of red azo dye onto bone char.
 Experiment 400-3-50. Temperature= 25 °C, pH=7, stirring rate=50 rpm, bone char
 mass=3.0002 g

Time (min)	Concentration (mg/l)	ϕ_{exp}
0	405.71	1
1	387.39	0.9548
30	374.68	0.9235
60	373.60	0.9209
127	371.22	0.9150
180	366.60	0.9036
362	364.70	0.8989
680	354.54	0.8739
1434	352.01	0.8676
2940	339.31	0.8363

Table 11. Experimental data of concentration decay of red azo dye onto bone char. Experiment 400-3-75: Temperature= 26.5 °C, pH=7, stirring rate=75 rpm, bone char mass=3.0001 g

Time (min)	Concentration (mg/l)	ϕ_{exp}
0	400.05	1
1	385.12	0.9627
30	385.12	0.9627
60	376.89	0.9421
120	374.99	0.9373
180	366.13	0.9152
352	363.60	0.9089
1440	351.58	0.8788
2790	341.45	0.8535

Figures 8 to 10 show graphically the decay concentration curves according to the initial conditions variable tested.

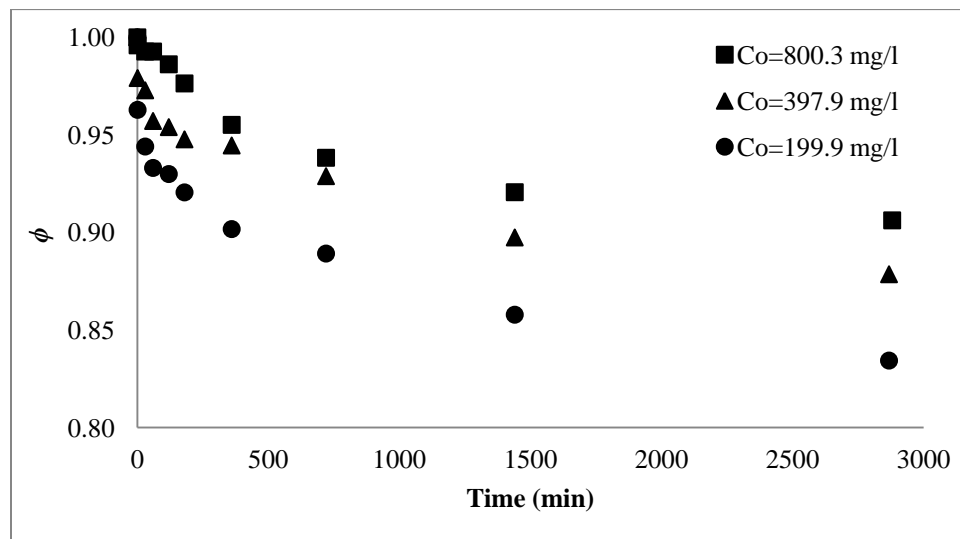


Figure 8. Concentration decay curves for adsorption of red azo dye onto bone char at three different initial concentrations. Bone char mass = 2 g, stirring rate=100 RPM, average temperature=24 °C, pH=7

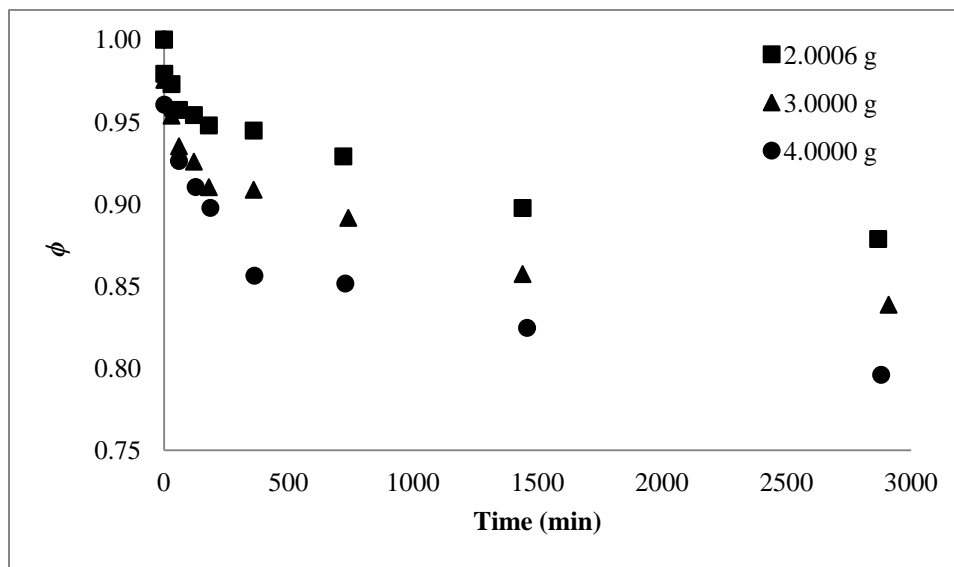


Figure 9. Concentration decay curves for adsorption of red azo dye onto bone char at three different bone char mass. Approx initial concentration = 400 mg/l, stirring rate=100 RPM, average temperature=25 °C, pH=7

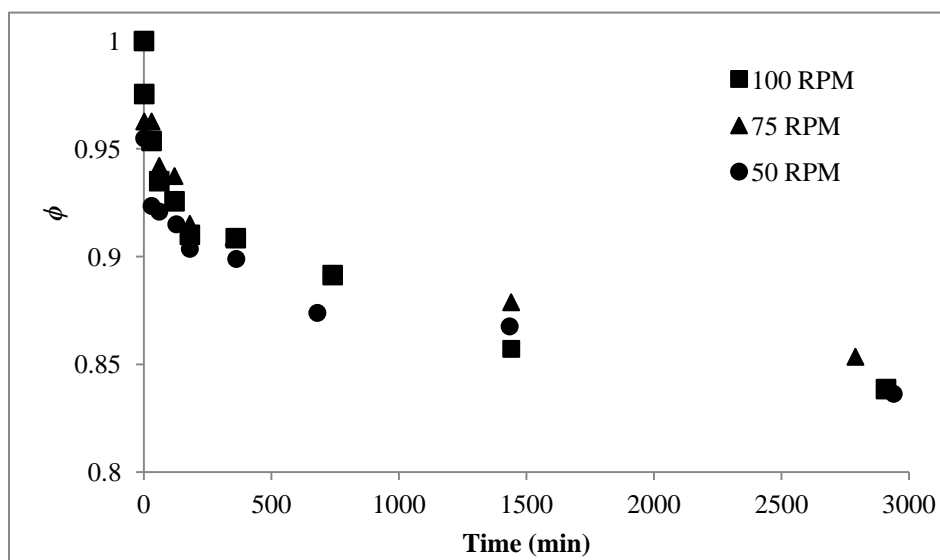


Figure 10. Concentration decay curves for adsorption of red azo dye onto bone char at three stirring speed. Initial concentration = 400 mg/l, bone char mass=3 g, average temperature=25 °C, pH=7

CHAPTER 6: CALCULATIONS, RESULTS AND DISCUSSION

In this section, the calculations made to obtain the diffusivities as results and the discussion of each section is found.

6.1. Equilibrium data

Bernal (2011) showed that the equilibrium behavior for the system red azo dye – bone char - water is well represent by Freundlich (1926) isotherm in the range studied in this project. The relation is showed by the Equation 6.1.

$$q_e = 24.778C_e^{1/4.213} \quad (6.1)$$

Where:

q_e : Solute mass adsorbed at equilibrium, mg/g

C_e : Bulk concentration at equilibrium, mg/l.

6.2. External mass coefficient calculation

According to Bernal & Leyva (2005), external mass transport coefficient can be estimated from the Equation 3.4.

$$V \frac{dC_A}{dt} = -mSk_c(C_A - C_{AS}) \quad (3.4)$$

When $t = 0$ min, $C_{A,r} = 0$ and $C_A = C_{A0}$, so it is possible to obtain Equation 6.2.

$$V \left. \frac{dC_A}{dt} \right|_{t=0} = -mSk_c C_{A0} \quad (6.2)$$

Rearranging, the Equation 6.3 can be developed.

$$k_c = -\frac{V}{mSC_{A0}} \left. \frac{dC_A}{dt} \right|_{t=0} = \frac{V\rho_P R}{3C_{A0}m} \left. \frac{dC_A}{dt} \right|_{t=0} \quad (6.3)$$

In order to calculate $\left. \frac{dC_A}{dt} \right|_{t=0}$, the slope of the concentration decay curve was estimated at $t = 0$, using then the first two points for each experimental set ($t = 0$ and $t = 1$). Figure 11 shows graphically the procedure for the experiment 400-2-100 and Equation 6.4 illustrates the calculation.

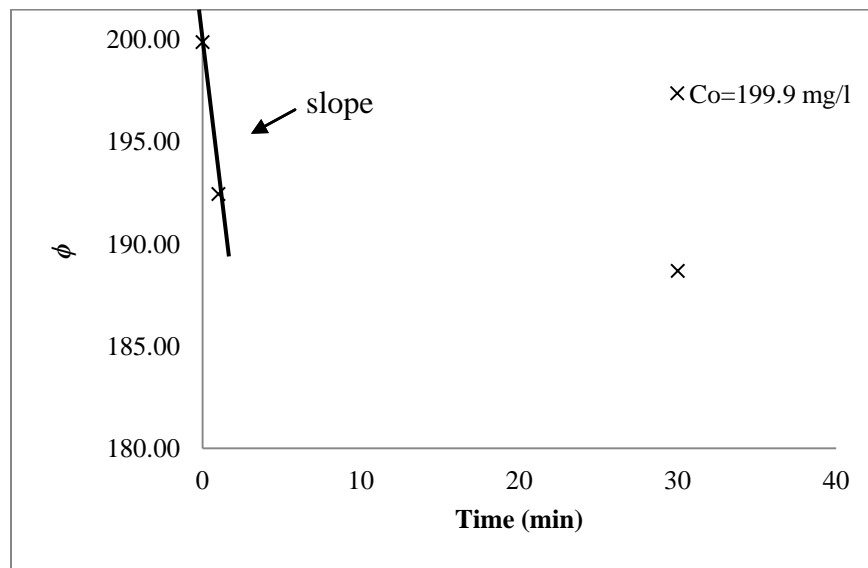


Figure 11. Slope of the first to points calculated to estimate the external mass transport coefficient for the experiment 400-2-100

$$\left. \frac{dC_A}{dt} \right|_{t=0} = \frac{C_{A1} - C_{A0}}{t_1 - t_0} = -0.1238 \frac{mg}{l.s} \quad (6.4)$$

Table 12 shows the results of the external mass transfer coefficient (k_c) for each experiment carried out.

Table 12. External mass transfer coefficient calculated for each experiment

Experiment	k_c (cm/s)
800-2-100	0.00041
400-2-100	0.00209
200-2-100	0.00372
400-3-100	0.00164
400-4-100	0.00198
400-3-50	0.00249
400-3-75	0.00301

The external mass transfer coefficient has a range from 0.00041 cm/s to 0.00372 cm/s, which means that, this value varies with initial conditions. All the experiments with initial concentration of 400 mg/l have a k_c around 0.002 mg/l, except the experiment 400-3-75, which has a $k_c=0.00301$ cm/s. Also, k_c seems to increase while the initial concentration decreases. Changes in bone char mass and stirring speed seem not to affect the k_c in the studied range.

6.3. External mass transport coefficient effect on the system

Figure 10 (Chapter 5) shows that the effect of the stirring speed (which has a direct relation with the external mass transport) can be neglected. That means that this parameter does not affect in a substantial way the adsorption rate.

Also, Figure 12 shows how the model predicts a change of k_c for the system. It is possible to see that the external mass transfer coefficient change very slightly the concentration decay curve. The major variation is observed for an order of magnitude of 10^{-2} . Nevertheless, the variation is not big. For orders of magnitude from 10^{-3} to 10^{-4} , the variation is very little. Table 12 shows that the variation of k_c for the experiments performed were between the latter orders of magnitude mentioned.

Because of this, the values of k_c for each experiment are conserved and applied with the respective diffusivities, according to the model tested.

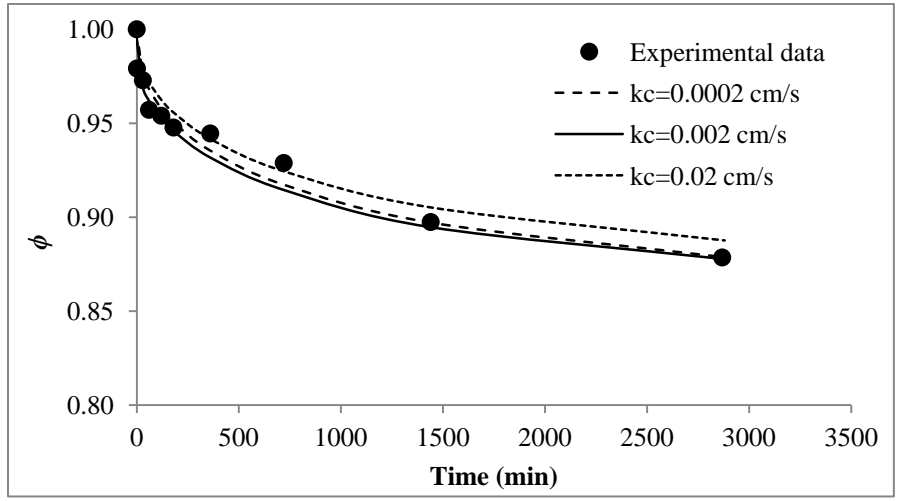


Figure 12. Effect of the external mass coefficient in the non-dimensional concentration decay curve for the experiment 400-2-100

6.4. Diffusivities calculation

In the methodology section was described the procedure to obtain the effective surface diffusivity and the effective pore diffusivity for each model tested. In this section, an **example** of the selection of the diffusivities is shown. Also, the results for each model tested are presented. The Figure 12 shows the three different values for $D_{e,s}$, fixing $D_{e,p}$ to a value of 3×10^{-8} for the experiment 400-2-100.

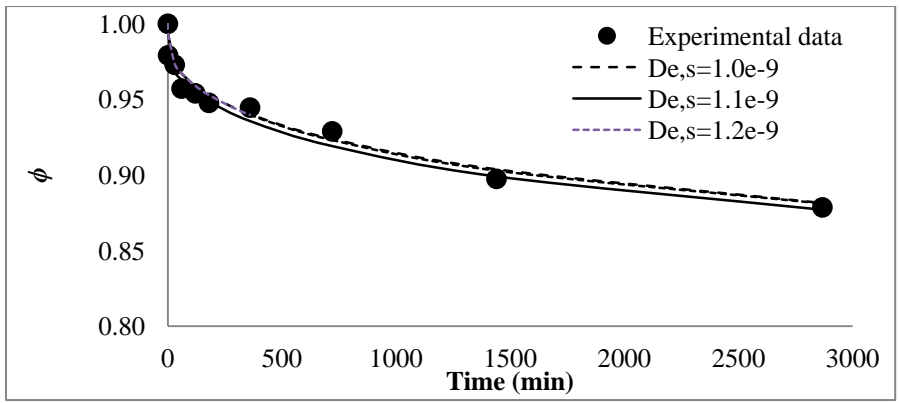


Figure 13. Effective surface diffusivity calculation for the experiment 400-2-100, fixing $D_{e,p} = 3 \times 10^{-8}$.

The $D_{e,s}$ value, which gives the least ARE is 1.1×10^{-9} . This can be observed in the Table 13.

Table 13. Average relative error for several effective surface diffusivities for the experiment 400-2-100, fixing $D_{e,p} = 3 \times 10^{-8}$.

$D_{e,p}$ (cm ² /s)	$D_{e,s}$ (cm ² /s)	ARE
3×10^{-8}	1.00×10^{-8}	0.668%
	1.09×10^{-10}	0.661%
	1.10×10^{-10}	0.562%
	1.11×10^{-10}	0.657%
	1.20×10^{-10}	0.638%

Then $D_{e,p}$ value obtained for each experiment was chosen by the same criterion as $D_{e,s}$ value (Table 14)

Table 14. Average relative error for several effective pore diffusivities for the experiment 400-2-100

$D_{e,p}$ (cm ² /s)	$D_{e,s}$ (cm ² /s)	ARE
2.5×10^{-8}	2.0×10^{-9}	0.578%
2.9×10^{-8}	1.5×10^{-9}	0.564%
3.0×10^{-8}	1.1×10^{-10}	0.562%
3.1×10^{-8}	1.0×10^{-9}	0.585%
3.5×10^{-8}	8.0×10^{-10}	0.592%
4.0×10^{-8}	4.7×10^{-10}	0.671%

In the case of Film-pore diffusion model and Film-surface diffusion model, it was not necessary to fix one of the parameters, since only one parameter was set.

6.4.1. Film-pore diffusion model (FPD)

The results of the effective pore diffusivity and the *Overall ARE* for the FPD model are shown in the Table 15. It can be observed that, the least *Overall ARE* for the FPD model is obtained with a global effective diffusivity of $D_{e,p} = 1.60 \times 10^{-8}$.

Table 15. Effective pore diffusivity and *Overall ARE* for FPD model

Experiment	$D_{e,p}$	<i>Overall ARE</i>
800-2-100	1.30×10^{-8}	2.131 %
400-2-100	1.80×10^{-8}	2.136 %
200-2-100	2.20×10^{-8}	2.134 %
400-3-100	1.60×10^{-8}	1.775 %
400-4-100	1.80×10^{-8}	2.136 %

Figures 14 and 15 illustrate the effect of the initial concentration and the bone char mass, respectively, in the system. There is a good fit for some cases. However, it is possible to see that some experiments are not good enough fitted, even when the *Overall ARE* is low. This is because, there is an excellent individual fit for some experiments and they low the average, but the fit with the same values for other experiments might be poor

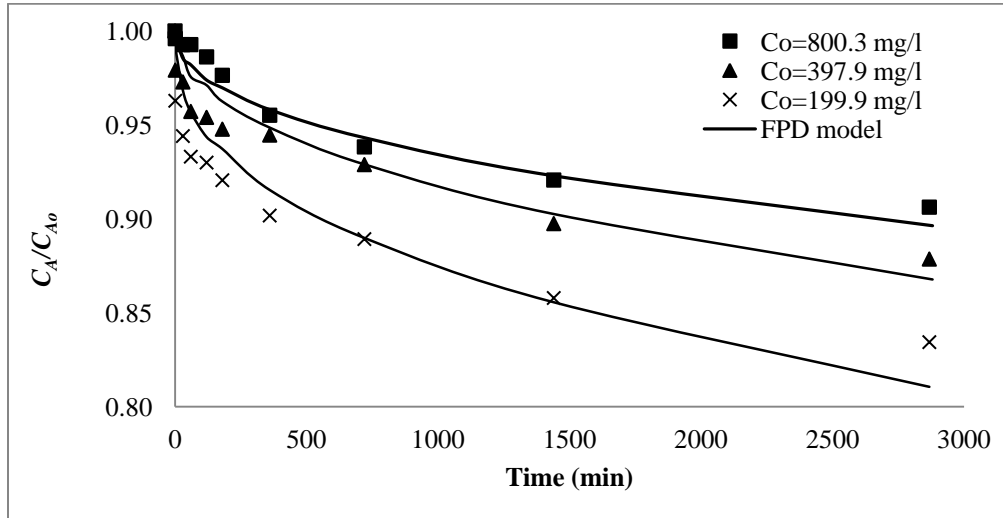


Figure 14. Effect of Initial concentration, FPD model, $D_{e,p} = 1.60 \times 10^{-8}$.
Bone char mass = 2 g, 25°C, pH=7, 100 rpm

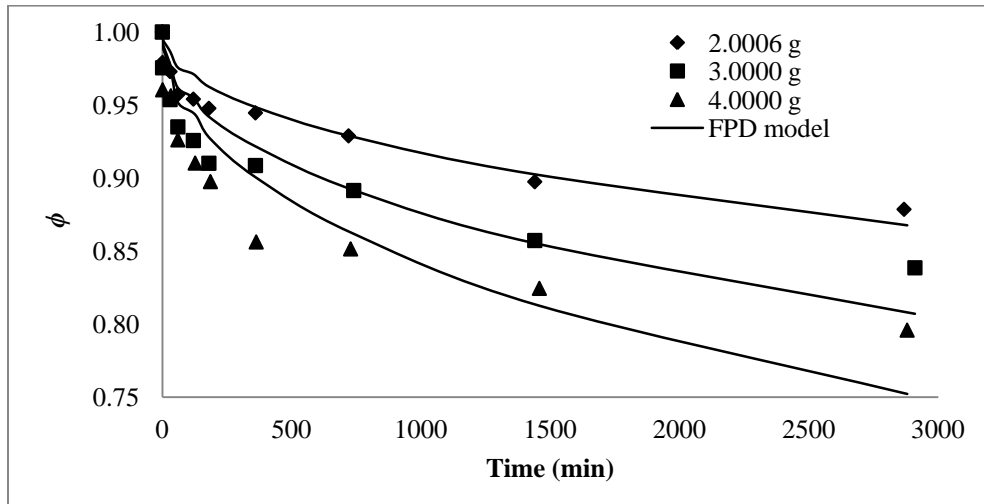


Figure 15. Effect of bone char mass, FPD model, $D_{e,p} = 1.60 \times 10^{-8}$.
Initial concentration = 397.9 mg/l, 25°C, pH=7, 100 rpm

6.4.2. Film-Surface diffusion model (FSD)

It can be seen on Figure 16 that, fit for FSD model for experiment 800-2-100 was not possible. This was enough to discard this model and to conclude that effective pore diffusivity is important to the system studied.

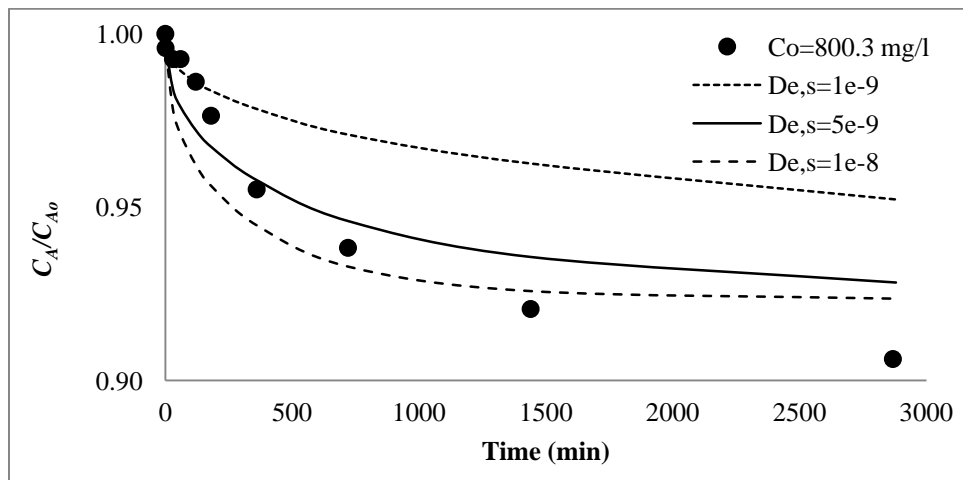


Figure 16. Different values of effective surface diffusivity (FSD model) for experiment 800-2-100. At 25 °C and pH 7

6.4.3. Film-pore-surface diffusion model (FPSD)

iii. Unique $D_{e,s}$ value (FPUSD)

Table 16 shows the value of effective pore diffusivity and the effective surface diffusivity found for each experiment, and the respective Overall Average Relative Error. The couple of diffusivities, which makes the model to fit the best are those from the Experiment 400-4-100. These values are:

Table 16. External mass transport coefficient, effective pore diffusivity and effective surface diffusivity for FPUSD model

Experiment	k_c (cm/s)	$D_{e,p}$ (cm ² /s)	$D_{e,s}$ (cm ² /s)	Overall ARE
800-2-100	0.00041	5.3×10^{-8}	9.6×10^{-10}	1.471%
400-2-100	0.00209	3.0×10^{-8}	1.1×10^{-9}	1.267%
200-2-100	0.00372	1.5×10^{-8}	7.5×10^{-10}	1.934%
400-3-100	0.00164	2.2×10^{-8}	1.9×10^{-9}	1.515%
400-4-100	0.00198	1.6×10^{-8}	1.5×10^{-9}	1.171%

All the *Overall Average Relative Errors* are lower than 2%, which denote good fit for most of the experiments. Also, in Table 17, it is possible to observe that the individual *ARE* using the diffusivities values selected are actually good fits for the system.

Table 17. External mass transfer coefficient, effective pore and surface diffusivities and Average Relative Errors for all the experiments with the chosen pair of diffusivities

Experiment	k_c cm/s)	$D_{e,p}$ (cm ² /s)	$D_{e,s}$ (cm ² /s)	ARE
800-2-100				1.355%
400-2-100				0.818%
200-2-100				1.387%
400-3-100	0.00198	1.6×10^{-8}	1.5×10^{-9}	1.681%
400-4-100				1.178%
400-3-50				1.253%
400-3-75				1.304%

Figure 17 shows the FPUSD model fit for the experiments with initial concentration variation and Figure 18 represents the model fit for the experiments with the bone char mass variation. It can be observed that, there are acceptable fits for experiments 400-2-100 and 200-2-100. Nevertheless, for the experiment 800-2-100 the fit seems to be not quite exact, especially after the minute 360, even though individual *AREs* are relatively low. Experiments with initial bone char mass of 2 g and 4g are also overestimated by this model.

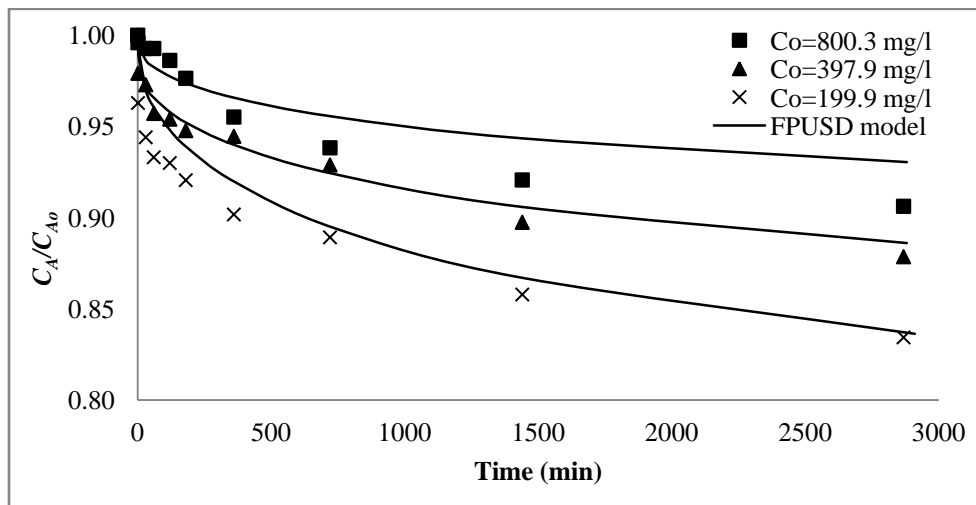


Figure 17. Effect of initial concentration, FPUSD model, $D_{e,p} = 1.6 \times 10^{-8}$ and $D_{e,s} = 1.5 \times 10^{-9}$. Bone char mass 2 g approx., 25°C, pH=7, 100 rpm

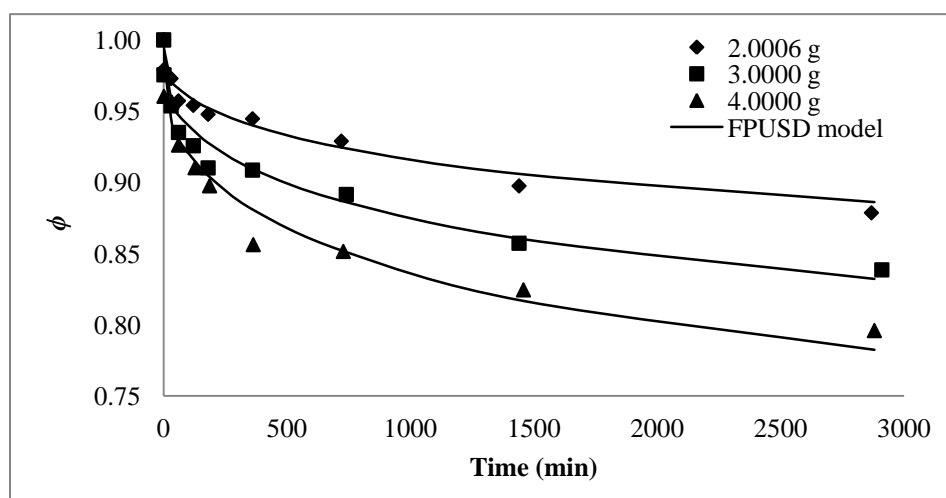


Figure 18. Effect of initial concentration, FPUSD model, $D_{e,p} = 1.6 \times 10^{-8}$ and $D_{e,s} = 1.5 \times 10^{-9}$ Initial concentration = 397.9 mg/l, 25°C, pH=7, 100 rpm

iv. Film-pore-initial condition dependent surface diffusion model (FPICDSD)

For the FPICDSD model, Table 18 shows the results for each experiment using the best fit value of the others and varying the effective surface diffusivity. The best $D_{e,p}$ value, which gives the least *Overall ARE*, is 1.60×10^{-8} . This value is also the least *Overall ARE* obtained for all the models.

Table 18. Pairs of diffusivities values for experiments and its respective *Overall ARE*

Experiment	$D_{e,p}$ (cm ² /s)	$D_{e,s}$ (cm ² /s)	<i>Overall ARE</i>
800-2-100		9.6×10^{-10}	
400-2-100		1.2×10^{-9}	
200-2-100	5.3×10^{-8}	1.5×10^{-9}	1.409%
400-3-100		1.2×10^{-9}	
400-4-100		2.4×10^{-9}	
800-2-100		3.1×10^{-9}	
400-2-100		1.1×10^{-9}	
200-2-100	3.0×10^{-8}	1.5×10^{-9}	1.070%
400-3-100		8.0×10^{-10}	
400-4-100		1.1×10^{-9}	
800-2-100		5.4×10^{-9}	
400-2-100		3.1×10^{-9}	
200-2-100	1.5×10^{-8}	7.5×10^{-10}	1.090%
400-3-100		3.0×10^{-9}	
400-4-100		1.9×10^{-9}	
800-2-100		2.0×10^{-9}	
400-2-100		4.0×10^{-10}	
200-2-100	2.2×10^{-8}	1.9×10^{-9}	1.149%
400-3-100		1.9×10^{-9}	
400-4-100		1.8×10^{-9}	
800-2-100		5.3×10^{-9}	
400-2-100		2.7×10^{-9}	
200-2-100	1.60×10^{-8}	2.0×10^{-9}	0.988%
400-3-100		2.4×10^{-9}	
400-4-100		1.5×10^{-9}	

Figures 19 and 20 show the model fit to the experimental data with the values selected for FPICDSD model. Again, experiment 800-2-100 has a not very good fit. It is possible, that

the cause of this could be that the concentration is too high and the system has a different behavior at high concentration.

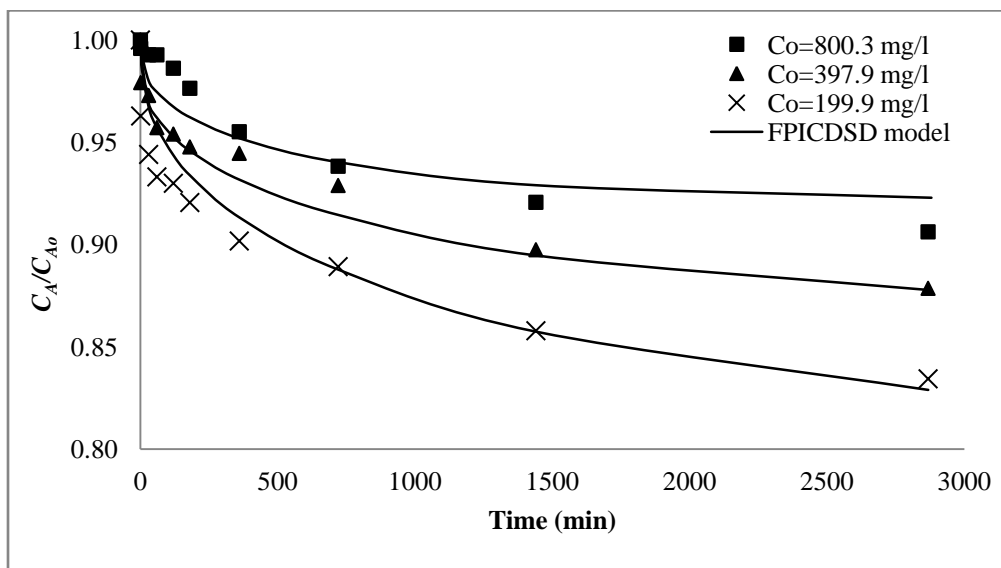


Figure 19. Effect of initial concentration, FPICDSD model, $D_{e,p} = 1.6 \times 10^{-8}$ Bone char mass 2 g approx., 25°C, pH=7, 100 rpm

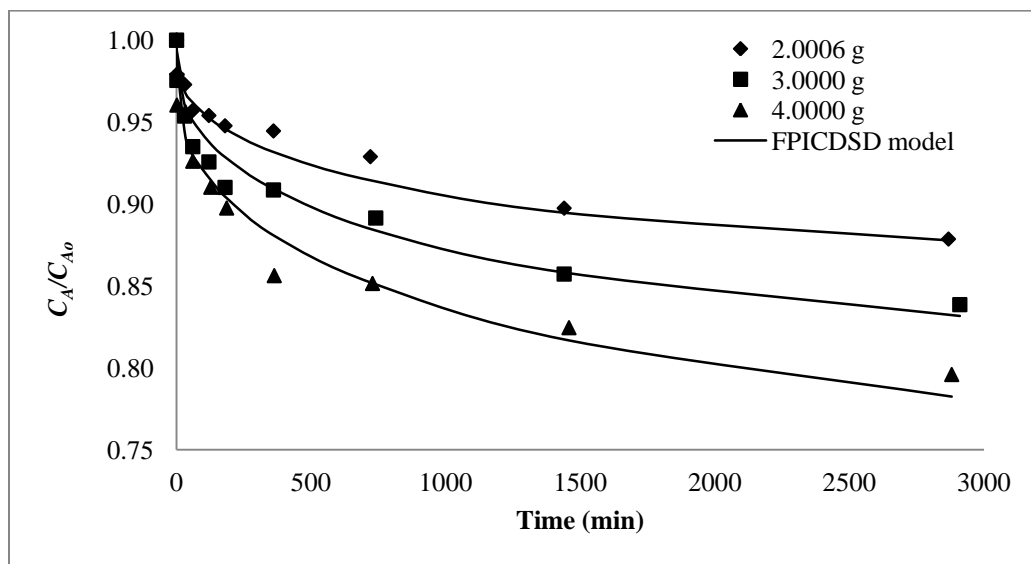


Figure 20. Effect of bone char mass, FPICDSD model, $D_{e,p} = 1.6 \times 10^{-8}$ Initial concentration = 397.9 mg/l, 25°C, pH=7, 100 rpm

It can be observed on Table 19 that, for the FPICDSD model, the effective surface diffusivity increases with the adsorbed mass at equilibrium (q_{∞}).

Table 19. Effective surface diffusivities obtained for FPICDSD model and equilibrium adsorbed mass for each experiment

Experiment	$D_{e,s}$ (cm ² /s)	q_{∞} (mg/g)
800-2-100	5.3×10^{-9}	112.01
400-2-100	2.7×10^{-9}	89.10
200-2-100	2.0×10^{-9}	66.96
400-3-100	2.4×10^{-9}	82.17
400-4-100	1.5×10^{-9}	74.32

Several studies (Bernal & Leyva, 2005), (Choy, et al., 2004), (Mollah & C.W., 1996) have reported that, in a model such as FPICDSD model, effective surface diffusivity $D_{e,p}$ is dependent of the adsorbed solute mass at equilibrium and proposed Equation 6.5 for this relation.

$$D_{e,s} = D_{s0} e^{q_{\infty}} \quad (6.5)$$

Plotting $\ln(D_{e,s})$ vs. q_{∞} (Figure 21), it is possible to see that the data seem to follow the trend of Equation 24.

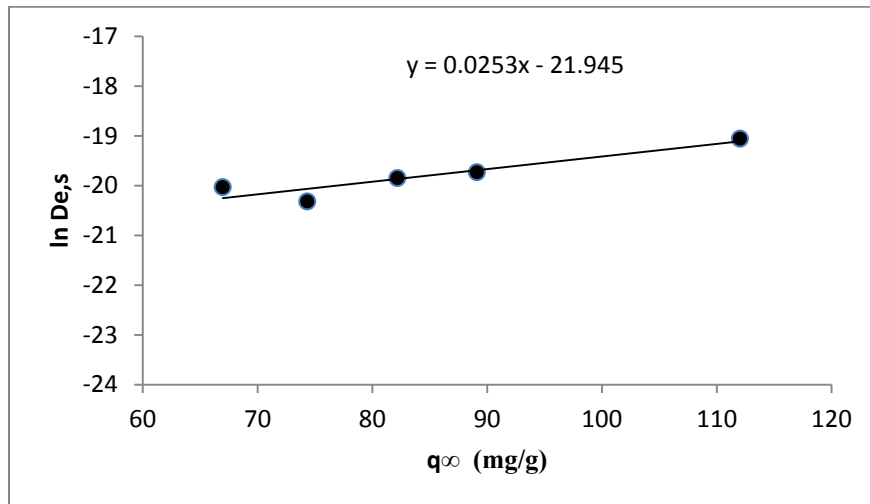


Figure 21. Linearized form of the Equation 24 for the experimental data

CHAPTER 7: CONCLUSIONS

The experiments were carried out successfully and the experimental data set for each initial condition was obtained.

The procedure for the estimation of the external mass coefficient seems to be correct. The results suggest that this coefficient increases while initial concentration decreases and changes in bone char mass and stirring speed appear not to affect it. However, the external mass transfer coefficient does not influence the behavior of the concentration decay curve in a significant way in the range studied.

It was demonstrated that, effective pore diffusion is important for the system studied. If effective pore diffusion is added to the model, the values of Average Relative Errors diminish.

In general, the Average Relative Errors and the Overall Average Relative Errors were low. The best fit was found for the Film- Pore- Initial Conditions Dependent Surface Diffusion (FPICDSD) model.

The best fit for all the experiments was achieved with the next parameter values:

Experiment	k_c (cm/s)	$D_{e,p}$ (cm ² /s)	$D_{e,s}$ (cm ² /s)
800-2-100			5.3×10^{-9}
400-2-100			2.7×10^{-9}
200-2-100	0.00198	1.6×10^{-8}	2.0×10^{-9}
400-3-100			2.4×10^{-9}
400-4-100			1.5×10^{-9}

The fit with these parameters gave as result Overall Average Relative Errors lower than 1.5%, which means a good fit. Nonetheless, for the experiment 800-2-100 seems to be a bigger difference between experimental data and model. A possible explanation for this is that, the initial concentration around 800 mg/l was high and the system might be behaving differently because of that. The rest of the experimental data was successfully fitted with the parameters showed, which indicates that they can be used for future calculations.

Also, it was found out that the effective surface diffusivity is dependent on the solute adsorbed mass at equilibrium. This is an exponential relation.

REFERENCES

Allen, S. & Koumanova, B., 2005. Decolourisation of water/wastewater using adsorption (review). *Journal of the University of Chemical Technology and Metallurgy*.

Atkins, P. & De Paula, J., 2003. *Fisicoquímica*. Madrid: McGraw Hill.

Bernal, L., 2011. *Estudio de equilibrio de adsorción del Rojo Remazol en carbón de hues*. San Luis Potosí: Universidad Autónoma de San Luis Potosí.

Bernal, L. & Leyva, R., 1999. *Adsorción y difusión intraparticulard de Zinc (II) en solución acuosa sobre carbón activado*. San Luis Potosí: Facultad de Ciencias Químicas, Universidad Autónoma de San Luis Potosí.

Bernal, L. & Leyva, R., 2005. *Equilibrio y cinética de adsorción de compuestos tóxicos sobre diferentes adsorbentes.* San Luis Potosí: Facultad de Ciencias Químicas, Universidad Autónoma de San Luis Potosí.

Cheung, W., Szeto, Y. & McKay, G., 2006. *Intraparticle diffusion processes during acid dye adsorption onto chitosan*, Hong Kong: Department of Chemical Engineering, Hong Kong University of Science and Technology.

Choy, K., Porter, J. & McKay, G., 2004. Film-surface diffusion during the adsorption of acid dyes onto activated carbon. *J. Chem. Technol. Biotechnol.*, Volumen 79, pp. 1181-1188.

Dudamel, W., Wolbert, D. & Cazeaudumec, Y., 2010. Modelado de la cinética de adsorción de plaguicidas en fase acuosa sobre carbón activado considerando efectos de la temperatura. *INTERCIENCA*, 35(4).

Freundlich, H., 1926. *Colloid and Capillary Chemistry*. 1st ed. London: Methuen and Co. Ltd.

Hines, A. & Maddox, R., 1987. *Trnasferencia de Masa: fundamentes y aplicaciones*. 2nd ed. Ciudad de México: Prentice Hall.

Ho, Y. & McKay, G., 1998. Sorption of dye from aqueous solution by peat. *Chemical Engineering Journal*, 2(70), pp. 115-124.

Lüth, H., 2010. *Solid surfaces, interfaces and thin films*. 5th ed. Heidelberg: Springer editoriañ.

Martínez, e. a., 2011. *Degradación del colorante azo rojo RR-272 presente en aguas contaminadas con un bio-electro-reactor de lecho fijo*, Querétaro: Intituto Tecnológico de Oaxaca y Centro de Investigación y Desarrollo Tecnológico en Electroquímica de Querétaro.

Mollah, A. & C.W., R., 1996. Pentachlorophenol adsorption and desorption characteristics of granular activated carbon-II. *Kinetics Wat. Res.*, 30(12), pp. 2901-2906.

Qiu, e. a., 2009. Critical review in adsorption kinetic models. *Journal of Zheijang University*, 10(5), pp. 716-724.

Quezada, M. & Buitrón, G., s.f. *Biodegradación aerobia de colorantes tipo azo (Rojo Ácido 151)*, Ciudad de México: Coordinación de Bioprocesos Ambientales, Instituto de Ingeniería, UNAM.

Treybal, R., 2002. *Operaciones de Transferencia de Masa*. Ciudad de México: Mc Graw Hill.

Weber, J., 1972. *Physico-chemical processes for water quality control*. New York: Interscience.

Wittcoff, H. & Reuben, B., 1980. *Productos Químicos Orgánicos Industriales*, s.l.: Limusa Noriega Editores.

Wu, J., 2004. *Modeling adsorption of organic compounds on activated carbon - A multivariate approach*, Umea: Department of Chemistry, Umea University.

Zoolilinger, H., 2001. *Color Chemistry: Syntheses, Properties and Applicarions of Organic Dyes and Pignments*, 3rd: John Wiley and Sons.